atmosphere

MDPI

Article

Heatwaves in the Future Warmer Climate of South Africa

Innocent Mbokodo [1,2,*], Mary-Jane Bopape [1], Hector Chikoore [2,3], Francois Engelbrecht [4] and Nthaduleni Nethengwe [2]

1 South African Weather Service, Private Bag X097, Pretoria 0001, South Africa; Mary-Jane.Bopape@weathersa.co.za
2 Department of Geography and Geo-Information Sciences, University of Venda, Thohoyandou 0950, South Africa; 32945280@nwu.ac.za (H.C.); Nthaduleni.Nethengwe@univen.ac.za (N.N.)
3 Unit for Environmental Sciences and Management, North-West University, Vanderbijlpark 1900, South Africa
4 Global Change Institute, University of the Witwatersrand, Johannesburg 2050, South Africa; Francois.Engelbrecht@wits.ac.za
* Correspondence: Innocent.Mbokodo@weathersa.co.za

Received: 10 February 2020; Accepted: 30 March 2020; Published: 3 July 2020

Abstract: Weather and climate extremes, such as heat waves (HWs), have become more frequent due to climate change, resulting in negative environmental and socioeconomic impacts in many regions of the world. The high vulnerability of South African society to the impacts of warm extreme temperatures makes the study of the effect of climate change on future HWs necessary across the country. We investigated the projected effect of climate change on future of South Africa with a focus on HWs using an ensemble of regional climate model downscalings obtained from the Conformal Cubic Atmospheric Model (CCAM) for the periods 2010–2039, 2040–2069, and 2070–2099, with 1983–2012 as the historical baseline. Simulations were performed under the Representative Concentration Pathway (RCP) 4.5 (moderate greenhouse gas (GHG) concentration) and 8.5 (high GHG concentration) greenhouse gas emission scenarios. We found that the 30-year period average maximum temperatures may rise by up to 6 °C across much of the interior of South Africa by 2070–2099 with respect to 1983–2012, under a high GHG concentration. Simulated HW thresholds for all ensemble members were similar and spatially consistent with observed HW thresholds. Under a high GHG concentration, short lasting HWs (average of 3–4 days) along the coastal areas are expected to increase in frequency in the future climate, however the coasts will continue to experience HWs of relatively shorter duration compared to the interior regions. HWs lasting for shorter duration are expected to be more frequent when compared to HWs of longer durations (over two weeks). The north-western part of South Africa is expected to have the most drastic increase in HWs occurrences across the country. Whilst the central interior is not projected to experience pronounced increases in HW frequency, HWs across this region are expected to last longer under future climate change. Consistent patterns of change are projected for HWs under moderate GHG concentrations, but the changes are smaller in amplitude. Increases in HW frequency and duration across South Africa may have significant impacts on human health, economic activities, and livelihoods in vulnerable communities.

Keywords: South Africa; heatwaves; future climate; Conformal Cubic Atmospheric Model (CCAM)

1. Introduction

Characteristics of extreme temperature events are expected to change due to global warming/global mean temperature increases. A recent study indicated that by 2017 the global mean temperature had increased by 1 °C with respect to preindustrial levels [1]. A more recent report [2] indicated that a global mean increase of about 1.5 °C could be seen in the future. Previous studies (e.g., [3,4]) have shown that there is a positive trend in both daily minimum and maximum temperatures across South Africa.

Furthermore, other studies have shown that mean temperatures across the subtropics and central tropical Africa are rising at double the global rate (e.g., [5]). Changes in the characteristics of extreme weather and climate events have also been observed over recent decades (e.g., [6,7]). An increase in the frequency of heavy rainfall events has been observed across South Africa [6] as well as an increase in rainfall intensity over parts of the country [7]. A decrease in cold temperature extremes and an increase in warm temperature extremes have also been detected [8].

The characteristics of heatwaves (HWs) are expected to change due to global warming [9]. Previous studies have shown the global averages of HW frequency, duration, and intensity are increasing in association with the increasing global mean temperatures [10,11]. However, that may not necessarily be the case on a regional scale, as temperatures vary from place to place depending on factors such as latitude, elevation, or prevailing weather conditions. It has been noted that there is a considerable variation of HW impacts from region to region [12]. Although HWs have been extensively studied in regions such as continental Europe (e.g., [13,14]) and Australia (e.g., [15–17]), they have not received rigorous research attention in South Africa, even though they have devastating impacts on society and livelihoods. It was found that there is an increase in warm temperature extremes and a decrease in cold temperature extremes across South Africa [8], consistent with global trends.

HWs can have negative impacts ranging from decreased agricultural yields to human health problems. The occurrence of HWs may lead to illnesses, particularly in children and the elderly [18], which may result in an increase in mortality rates [19,20]. HWs can impact water supply through increased evaporation rates, and can also damage crops and vegetation. They may minimize crop production since environmental factors such as temperature and soil moisture are determinant factors of yields [21]. HWs can also affect the economy of a region through extensive usage of air conditioners as a mitigation strategy to heat stress [22].

Several studies have focused on longer lasting HWs (e.g., [13,23–25]), while other studies have investigated short-lived events (e.g., [26,27]). Short-lived HWs can also induce wildfires that can damage property, because they usually occur during droughts, due to enhanced subsidence and coinciding with dry vegetation. They can also impact on human livelihoods negatively through illnesses and deaths. In 1995, a HW which only lasted for 3 days killed about 700 people in Chicago in the United States [24]. The impacts of HWs on agriculture, the economy, and on human beings, and the high vulnerability of South African society to the impacts of extremely warm temperatures highlight the necessity to study the occurrence and nature of these events and their projected changes.

It has been indicated that health and climate change adaptation strategy discussions are often limited in South African sub-national governments [28]. This can partially be credited to the lack of research of other extreme events such as HWs. In depth knowledge about the projections of HWs in South Africa will assist several stakeholders in decision making to prepare appropriate mitigation and/or adaptation strategies which can minimize the associated negative impacts.

Previous studies (e.g., [15]) have indicated that regional climate models project an increase in duration, frequency, and intensity of extreme events for the 21st century. Garland et al. [29] showed that extreme apparent temperature days in Africa are projected to increase in the future climate using the Conformal Cubic Atmospheric Model (CCAM) forced with the A2 emission scenario, whilst Engelbrecht et al. [5] projected substantial increases in the annual number of HW days. The aim of this work was to analyze projections of HWs across South Africa using the CCAM over the period of 1983–2099 under the Representative Concentration Pathway (RCP) 4.5 and 8.5 emission scenarios with different greenhouse gas (GHG) concentrations. The CCAM model used in this study has high resolution and improved orography, and the forcing scenarios have been updated with respect to previous studies on similar models.

The subsequent sections discuss methods of analyses applied and results of this study. In the results, comparisons of simulated average maximum temperatures, HW thresholds, and variability are presented in relation to observations followed by HWs in future warmer climates and concluding remarks.

2. Data and Methods

The CCAM model was used to simulate present-day and future global climate for the period 1961–2099 with surface forcing from six different Global Climate Models (GCMs) forced by two different emission scenarios, namely RCP 4.5 and RCP 8.5. The CCAM was developed by the Commonwealth Scientific and Industrial Research Organization (CSIRO) in Australia [30,31] and is based on a conformal cubic grid with a semi-Lagrangian and semi-implicit dynamical core that solves hydrostatic primitive equations [32]. CCAM is a global model, but it can also be employed as a regional climate model (RCM) using stretched-grid variable-resolution mode [33,34]. CCAM includes a prognostic cloud scheme [35], a cumulus convection scheme with a mass-flux closure [36], the Geophysical Fluid Dynamics Laboratory (GFDL) parameterizations for long-wave and short-wave radiation, and a stability-dependent boundary layer scheme based on Monin Obukhov similarity theory with non-local treatment [37,38].

The CCAM model has here been integrated coupled to the CSIRO Atmosphere-Biosphere Land Exchange model (CABLE). The simulations used in this study were generated on a quasi-uniform global grid of about 50 km resolution in the horizontal and with the RCP 4.5 and RCP 8.5 to account for the uncertainty in the emission scenarios. The RCPs were developed by the Intergovernmental Panel on Climate Change (IPCC) in its Assessment Report Five (AR5), superseding the Special Report on Emissions Scenarios (SRES) [39]. RCP 4.5 represents a moderate GHG concentration future, whilst RCP 8.5 represents a high GHG concentration future. The CCAM model was forced with sea ice and sea surface temperatures from six earth system models (Table 1) under RCP 4.5 and RCP 8.5 forcing conditions and results in a total of 12 ensemble members were produced.

There are several definitions of HWs in different regions across the world. This work adopted the South African Weather Service (SAWS) definition that a HW is "when for at least three consecutive days the maximum temperature of a certain region or grid point is five degrees or higher than the average mean maximum for the hottest month for that particular station or grid point". This definition is similar to the one used in previous studies on HWs (e.g., [40]), while other studies prefer to define HWs as events of at least six consecutive days (e.g., [33]). There are several different thresholds used when defining a HW, based on weather conditions of the area being considered. The threshold used to identify HWs for all the present-day and future periods are based on the threshold that define HWs under present-day climate. Therefore, the definition used does not take into account possible changes in damage and impact due to adaptation. This definition also does not capture relatively extreme events occurring during the colder seasons that may not reach this extreme temperature threshold, but that could result in strong ecological impacts, such as affecting the growing season, and agricultural and ecological development. The definition of HWs used in this study will ensure that shorter-lived events are also detected. The use of a threshold linked to maximum temperature average for each location (grid point in the case of a model simulation) makes it possible for the HWs to vary based on the climatology of each region in South Africa.

Our analyses were split into 30-year averages, where the period 1983–2012 was considered as the present-day baseline, and the periods 2010–2039, 2040–2069, and 2070–2099 were considered as representing the near, mid, and far-future respectively. Simulations obtained from emission scenarios RCP 4.5 and RCP 8.5 are shown separately.

Three different measures of the characteristics of HWs were considered, namely, the frequency, duration, and intensity. Frequency was calculated as total actual occurrences per seasons per 30-year period while duration is the total number of days a HW lasts. The HW intensity was calculated using the average maximum temperature during all the days identified as forming part of the HW event.

The present-day simulations were compared with SAWS observations and also to HWs in future periods. The simulated HWs were identified using thresholds identified for each grid point after interpolation of the simulations to a 0.5° resolution latitude-longitude grid. Those obtained from the SAWS observations were identified for each station. South Africa has a good network of surface

temperature stations compared to other countries in southern Africa, however for this study 24 stations were selected countrywide (Figure 1) based on a 95% data availability criteria during the study period.

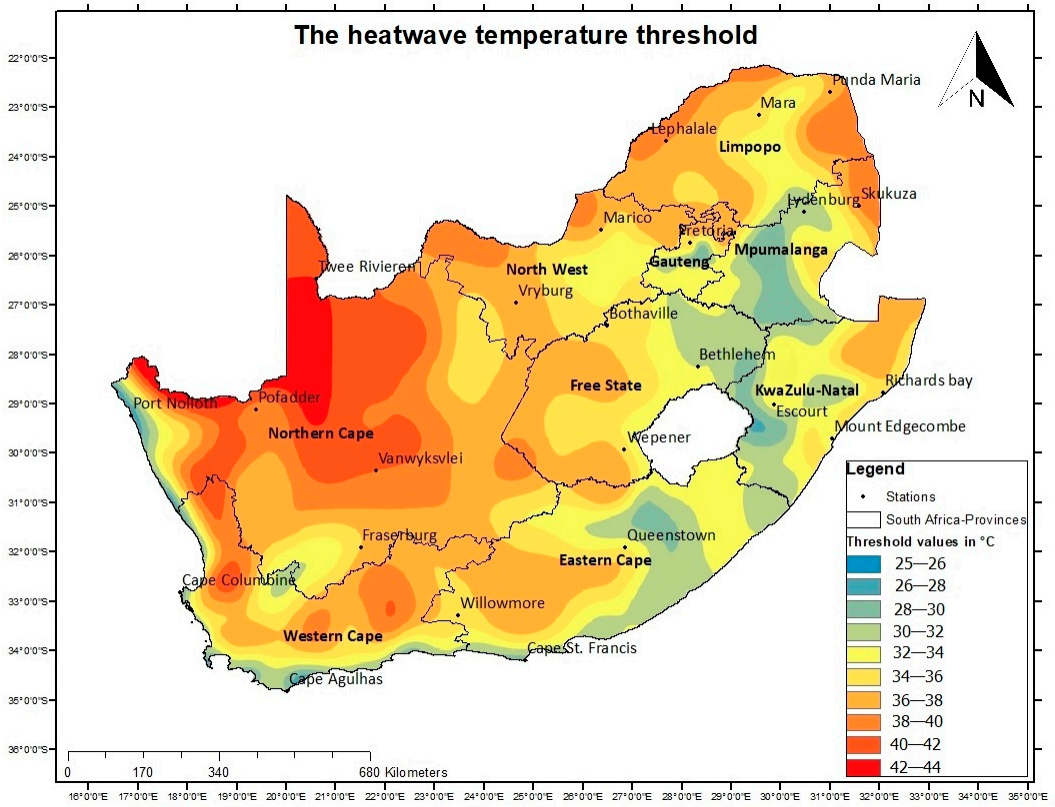

Figure 1. Twenty-four South African Weather Service (SAWS) stations used in this study with a 95% availability overlaid on the observed HW threshold (°C) used for warnings issued by SAWS.

RClimDex version 1.0 software [41] was used to quality control the weather station data. RClimDex is an R based statistical tool which is freely downloadable from the Expert Team on Climate Change Detenction, Monitoring and Indices (ETCCDMI) website [42] and outputs of this are shown in Tables 2 and 3. The next section will discuss the results starting with a comparison of simulated present-day events and observations. The projections for the three future periods will subsequently be discussed, followed by a discussion and concluding remarks.

Table 1. List of ensemble members used in this study. RCP—Representative Concentration Pathway.

Model	RCP 4.5	RCP 8.5
ACCESS 1-0 (BoM-CSIRO, Australia) [43]	✔	✔
CCSM4 (NCAR, USA) [44]	✔	✔
CNRM-CM5 (CNRM-CERFACS, France) [45]	✔	✔
GFDL-CM3 (NOAA, USA) [46]	✔	✔
MPI-ESM-LR (MPI, Germany) [47]	✔	✔
NorESM1M-M (NCC, Norway) [48]	✔	✔

Table 2. List of relevant ETCCDMI indices utilized in this study.

Index	Description	Units
Tx	Daily maximum temperature	°C
Tn	Daily minimum temperature	°C
Tn10P	Annual number of days when Tn < 10th percentile	days
Tn90P	Annual number of days when Tn > 90th percentile	days
Tx10P	Annual number of days when Tx < 10th percentile	days
Tx90P	Annual number of days when Tx > 90th percentile	days
DTR	Annual diurnal temperature range	°C

Table 3. Trend results for selected temperature indices from 1983 to 2012 (* indicates significance at the 95% level of confidence) and total number of heatwave (HW) occurrence per station.

Station Name	Tn10P (Days)	Tn90P (Days)	Tx10P (Days)	Tx90P (Days)	DTR (°C)	Total Number of HW Occurrences
Bethlehem	−0.063 *	0.092 *	−0.057 *	0.151 *	0.007	9
Bothaville	−0.324 *	0.077	−0.034	0.275 *	0.045 *	27
Cape Agulhas	−0.199 *	0.392 *	−0.199 *	0.392 *	0.01	0
Cape Columbine	−0.211 *	0.158 *	−0.046 *	0.141 *	0.001	15
Cape St. Francis	−0.067 *	0.165 *	−0.184 *	−0.107 *	0.031 *	6
Escourt	−0.127 *	0.108 *	−0.012	0.213	0.032 *	18
Fraserburg	−0.06	0.19 *	−0.04	0.244	0.003	6
Lephalale	−0.354	0.453 *	−0.155	0.834 *	0.052 *	27
Lydenburg	−0.163 *	0.052	−0.092 *	0.336 *	0.014	3
Mara	−0.322 *	0.027 *	−0.042	0.356 *	0.038 *	33
Marico	−0.186 *	0.113	0.148 *	0.027	0.006	36
Mount Edgecombe	−0.326 *	0.206 *	−0.019	0.176 *	0.008	0
Pofadder	−0.063	0.151 *	−0.012	0.186	−0.006	6
Port Nolloth	−0.116 *	0.018 *	−0.063 *	0.218 *	0.035 *	71
Pretoria	−0.314 *	0.049	−0.023	0.028	−0.005	6
Punda Maria	−0.438 *	0.116 *	−0.038 *	0.137 *	0.034 *	45
Queenstown	−0.329 *	0.208 *	−0.174 *	0.051	0.001	24
Richards bay	−0.339 *	0.283 *	−0.143 *	0.515 *	0.069 *	6
Skukuza	−0.283 *	0.109	−0.114 *	0.2	0.036 *	21
Twee Rivieren	−0.262 *	0.065 *	−0.122 *	0.832 *	0.111 *	12
Vanwyksvlei	−0.118 *	0.062	−0.076 *	0.091	0.018 *	6
Vryburg	−0.298 *	0.123 *	0.057 *	0.166 *	0.039 *	21
Wepener	−0.035 *	0.173 *	−0.18	0.1 *	−0.037 *	6
Willowmore	−0.117 *	0.305 *	−0.165 *	0.183 *	0.024 *	24

3. Results

3.1. Osberved vs. Simulated Average Daily Maximum Temperature (T_X) and HW Thresholds

Figure 2a shows the average observed maximum temperature across South Africa during mid-summer, December–February (DJF), for the period 1983 to 2012. Figure 2c shows the 50th percentile of the simulated average temperature for the RCP 4.5 scenario during the same period. The observed and simulated 30-year daily average maximum temperature indicate that South Africa experiences highest maximum temperatures during DJF across the northern parts of the country. The highest values are shown in the dry regions in the northwestern parts, with averages of over 36 °C. The model positions the highest temperature in the northwestern parts which is consistent with the observations. The model is able to capture the observed east–west and south–north temperature gradient, as well as the colder temperatures at higher altitudes across the Drakensberg Mountains in the eastern parts of the country. There are small differences amongst different ensemble members under both RCP 8.5 and RCP 4.5 in the present-day climate. Moreover, the RCP 8.5 and 4.5 emissions are similar until the year 2004, and only then start to diverge, however by the end of 2012 the differences between the two scenarios remain small. Figure 2b,d show the observed and simulated average maximum temperatures for mid-winter, June–August (JJA). Lower daily average maximum temperatures are observed in this season, and the model is also able to capture this seasonal variability. The observed and simulated temperatures average to less than 22 °C in much of the interior and coastal regions for winter during the 1983–2012 period.

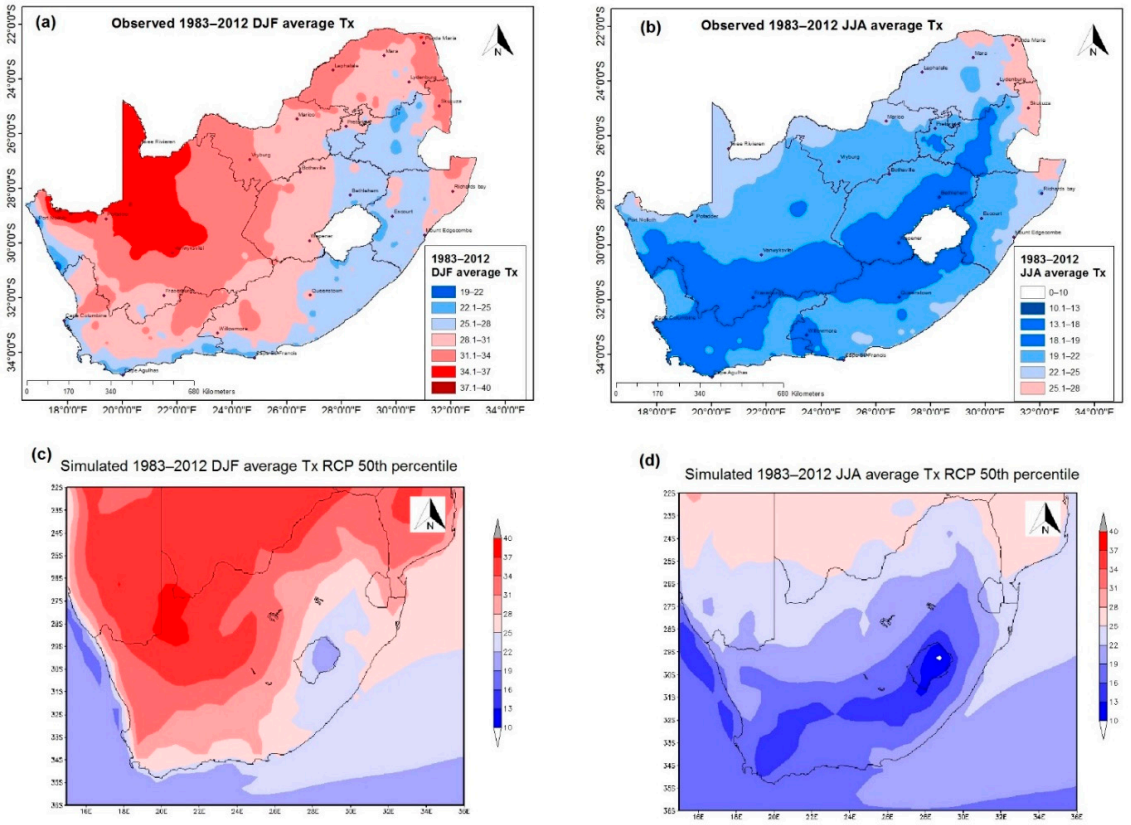

Figure 2. Observed 1983–2012 average Tx (°C) for (**a**) December–February (DJF) and (**b**) June–August (JJA) and simulations of 1983–2012 RCP 4.5 scenario 50% percentile average Tx (°C) for (**c**) DJF and (**d**) JJA.

Tables 2 and 3 show the list of indices and observed trends in extreme temperature events across South Africa with the Kendall's tau-based slope estimator used for the significance assessment.

The Tn10P and Tx10P columns in Table 3 show that there is a decreasing trend in the number of cold days. The two columns indicate that there is a decrease in the number of days associated with lower minimum and maximum temperatures, respectively. The negative trend is significant across 21 of the 24 selected stations for minimum temperatures, and 14 stations for maximum temperatures. The number of days associated with the highest minimum and maximum temperature were increasing at all the stations. For the maximum temperature, only Cape St Francis has a negative trend, which is statistically significant. These results are in agreement with studies that have shown a decrease in cold extreme events, and an increase in hot extreme events (e.g., [8]).

Daily average maximum temperatures are projected to increase by up to 2 °C during the period 2010 to 2039 as compared to the reference period of 1983 to 2012 during summer across the country's plateau (Figure 3a,b). Most central parts of the subcontinent are expected to experience increases of over 1 °C. Regions with projected temperature increases of more than 1 °C extend into the neighboring countries across the subtropical western parts of Africa for all RCP 8.5 projections. The winter temperatures are also projected to increase, with the median of the RCP 4.5 downscalings projecting increases of less than 1 °C across larger part of the central interior. The coastal areas are projected to have a lower increases as compared to inland.

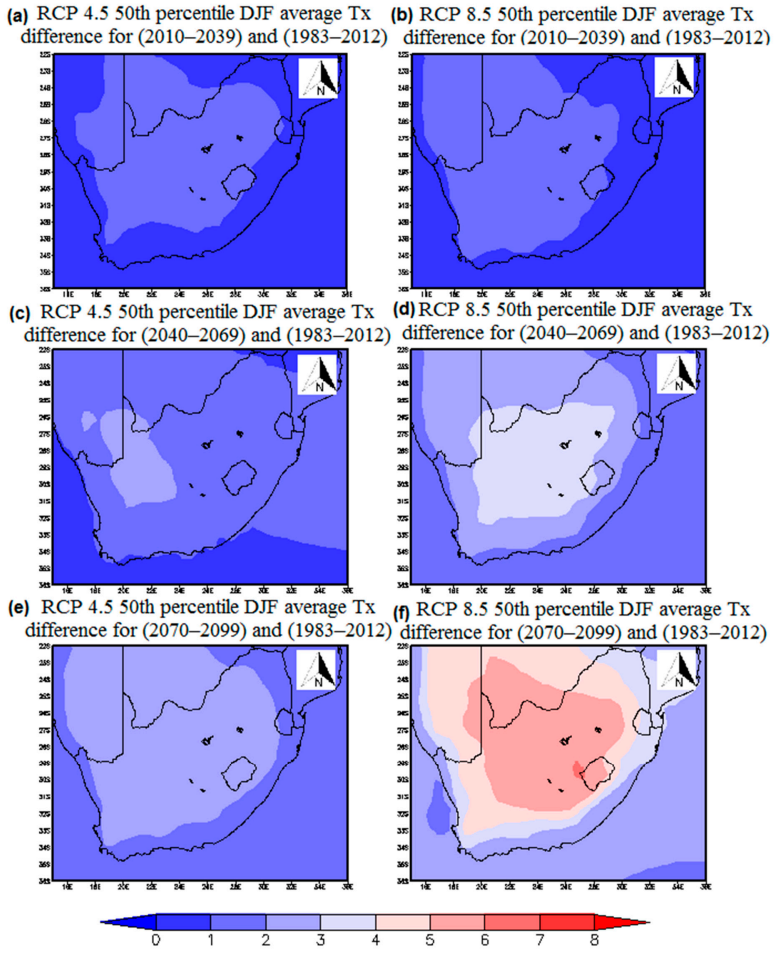

Figure 3. Simulations of DJF average Tx (°C) 50th percentile differences of average Tx (°C) difference between 1983 and 2012 with future climates: (**a**) 2010–2039 RCP 4.5, (**b**) 2010–2039 RCP 8.5, (**c**) 2040–2069 RCP 4.5, (**d**) 2040–2069 RCP 8.5, (**e**) 2070–2099 RCP 4.5 and (**f**) 2070–2099 RCP 8.

The projected temperature increases in the medium-term period of 2040–2069 are larger than those projected for the present-day/near term future period of 2010 to 2039 (Figure 3c,d). The RCP 8.5 projections show increases of over 3 °C on four provinces of South Africa and parts of Lesotho, which

is landlocked in South Africa and characterized by high altitudes. Projected temperature increases over the coastal regions are slower because of the moderating effects of the oceans.

The climate change signal is expected to be largest for the period 2070 to 2099 (Figure 3e,f), because it is the furthest and the anthropogenic greenhouse gas concentrations will be largest especially in the RCP 8.5 emission scenario. The summer temperatures are projected to rise further, with increases going in excess of 6 °C in the RCP 8.5 scenario for the period 2070–2099. The projected increase across the coastal regions is also smaller as with the, near future and medium-term projections. All the ensemble members, both in the RCP 4.5 and RCP 8.5, show an increase in temperature across the whole of South Africa, which indicates that there is a high confidence in the temperature projections. The increase in the mean temperatures are expected to have an effect on the characteristic of HWs in the future climate.

3.2. Observed vs. Simulated HWs

The SAWS definition of a HW was used, where all events with an observed or simulated temperature of 5 °C or greater above the daily average maximum temperature of the hottest month, for a minimum of three consecutive days, are identified, for each station or grid point, respectively. The threshold calculation is made based on present-day climate simulations, and the present-day thresholds are applied to future projections. These thresholds are used by the Disaster Risk Reduction (DRR) division of SAWS which issues HW warnings to the public. The HW thresholds are generally higher across the western parts of the country (which are also arid), ranging from 32 to 44 °C, in line with observed average temperatures shown in Figure 2a during DJF (when most HW are experienced). The thresholds are also relatively high in the north-east lowveld, ranging from 32 to 40 °C.

South Africa experiences a considerable spatial variability of HW occurrences seasonally (Figure 4). The country experienced higher HW frequency in the northern parts, with Punda Maria (22.68° S, 31.02° E) recording 45 HWs from 1983 to 2012. The north-eastern low-lying regions generally experience relatively high HW occurrences being warm throughout the year.

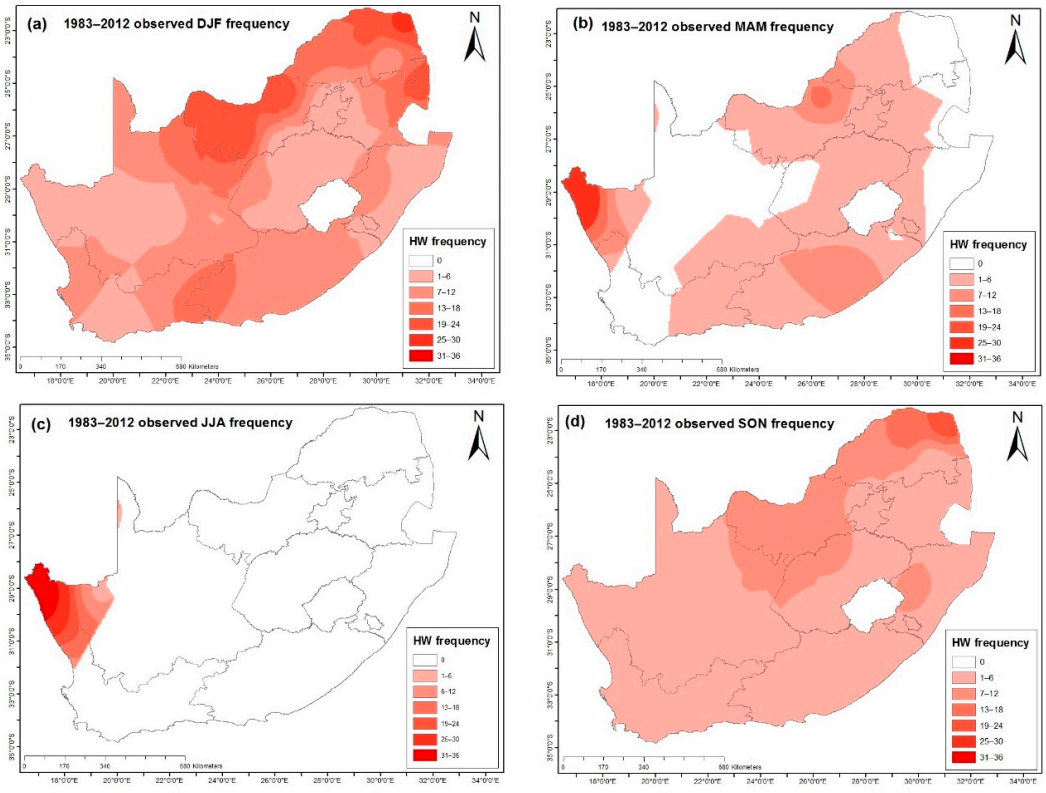

Figure 4. Observed HW frequency (total number of occurrence) across South Africa from 1983 to 2012 during (**a**) DJF, (**b**) March–May (MAM), (**c**) JJA and (**d**) September–November (SON).

Observations show that most regions experience HWs during the austral summer, particularly in DJF, with the exception of subtropical western to south-west coastal regions experiencing HWs mainly between May and August. The northern parts of South Africa generally experienced over 12 HWs between September and November (SON) during the period 1983–2012. The western coastal regions of South Africa experienced most HWs in winter when subtropical anticyclones are more equator-ward and when a continental high becomes more established. Descending offshore flow warms dry adiabatically creating a coastal low that precedes the arrival of a cold front during this time. This descending wind leads to berg winds and have been linked to frequent HW occurrences across the south coast of South Africa. Port Nolloth experienced most (71) HW occurrences between 1983 and 2012, 66 of which occurred between April and September. Figure 5a shows the observed average duration of the HWs across the whole of South Africa. The southern parts of the country are observed to experience shorter lived HWs. The extreme northern parts of Limpopo experience HWs that last for six days or more on average.

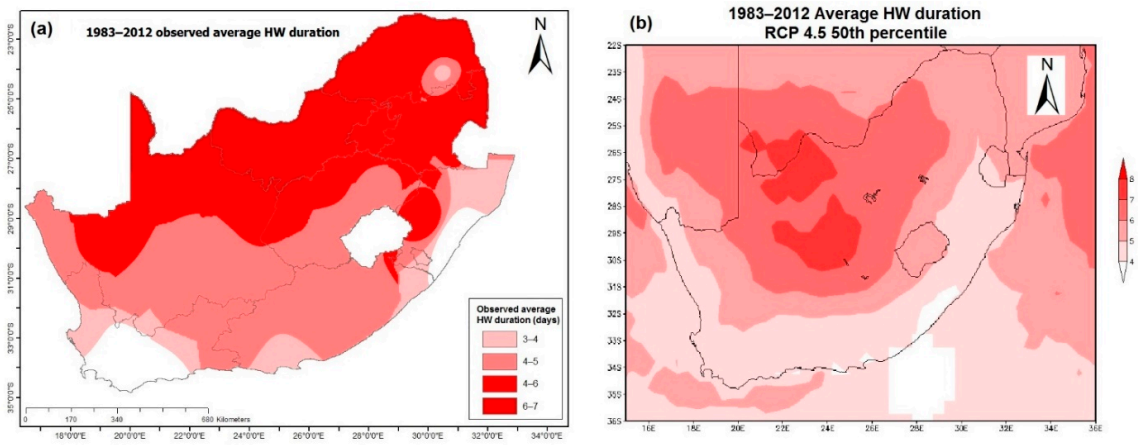

Figure 5. (**a**) Observed and (**b**) simulated HW average duration (days) across South Africa from 1983 to 2012.

Simulated thresholds were calculated for both RCP 4.5 and 8.5 for all ensemble members and were found to exhibit a similar pattern as the observations. Figure 6a,b show examples of these thresholds from one of the members, CCAM forced with CCSM4, for both RCP4.5 and RCP8.5. Simulated HW thresholds are well below 32 °C in much of the eastern parts and coastal regions of the country. The simulated HW thresholds for both RCP 4.5 and 8.5 are spatially consistent with the observed thresholds (Figure 1). The model shows an east–west and south–north gradient, with the highest thresholds in the north and the west as shown in the observations. The median HW frequency as simulated by CCAM is shown in Figure 6c,d for DJF and JJA, respectively. The number of HWs simulated across northern parts of the country is high for both RCPs, as well as across the interior regions adjacent to the south and east coasts. Figure 4a and b also show that SON and DJF are observed to have more HWs than other seasons. The CCAM model is able to capture the relatively large number of HWs across the Limpopo province. Across the western parts of the country, the largest number of HWs is simulated further west of where the events are observed to peak in frequency. The CCAM model is found to simulate a somewhat larger number of HWs than what is observed in general. It also had challenges simulating winter HWs over the west in the present-day climate.

Most parts of the country are observed to experience the smallest number of HWs during the winter season with an exception of north-western coast of South Africa where observed HWs are higher. This may be due to prolonged berg winds resulting from the anticyclonic flow by the Atlantic High which is more equator-ward during this time. The eastern part of the country is different, where simulations indicate relatively high number of HWs compared to observations in winter.

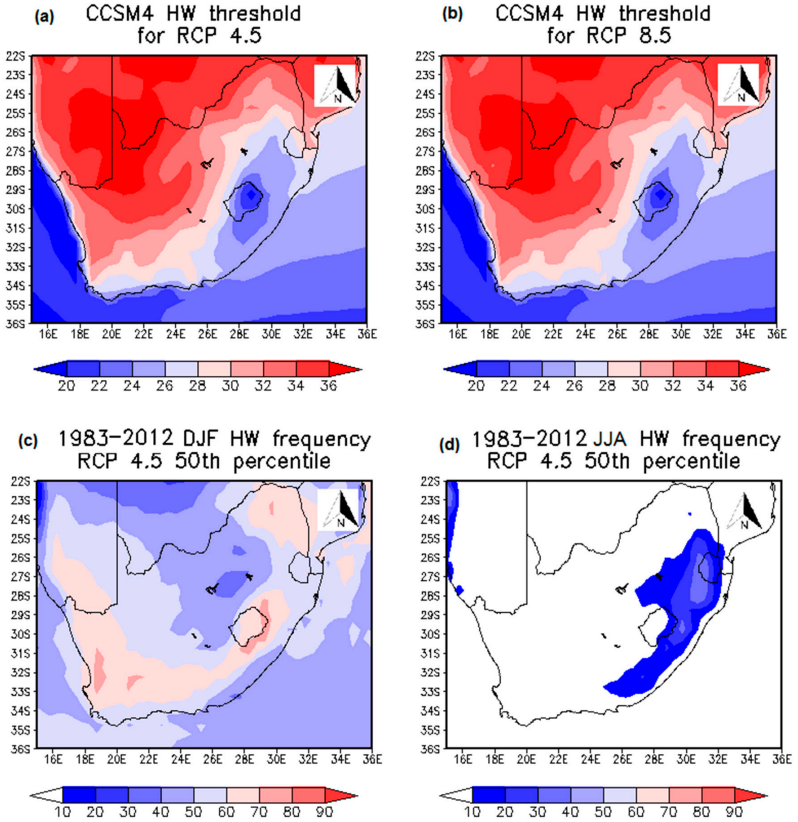

Figure 6. Simulations of HW thresholds (°C) for (**a**) CCSM4 RCP 4.5, (**b**) RCP 8.5 and RCP 4.5 scenario HW frequency (total number of occurrence) during the present-day climate, (**c**) 1983–2012 DJF and (**d**) JJA.

The CCAM model captures the seasonal differences in the number of HWs well. The smallest number of HWs is simulated to occur in winter, while the highest number is simulated for summer. The number of HWs simulated in spring is higher than those simulated for autumn, however, both autumn and spring HWs are fewer than those that occur in summer, and more than those that occur in winter. The spring simulations are in agreement with observations in that they show the highest number of HWs across the eastern parts of the country. The observations showed a similar seasonal cycle, and hence we can say the CCAM model simulates present-day climate with high skill, and its future projections can be considered with some confidence. The observed average HW duration was shown in Figure 5a. Figure 5b shows the simulated average duration for DJF and JJA for RCP 4.5 during the present-day climate. The south-north gradient is captured in general, with the southern parts of the country experiencing shorter lived HWs. However, the model does not capture the location of the longest lived HWs across the northern most parts of the country. It may be noted that the observed duration is based on only 24 stations across the whole of the country, while the peak in the north is a result of interpolating from two stations.

With a warming globe, the expectation is that HW characteristics may not be the same in future climate compared to those occurring in current climate. This is largely due to the fact that average temperatures are increasing, and hence the present-day thresholds for defining a HW may be exceeded easily. We analyzed the projected HWs using the present-day definition, because that is the definition that we experience in our current climate. Very long lasting HWs in the future climate may simply mean the average temperature has gotten higher, and perhaps what is considered as a HW in the current climate will not be considered as a HW in the future climate using future averages. The subsequent sections provide expected HW frequency, duration and intensity in South Africa in the future climates, i.e., 2010 to 2039, 2040 to 2069, and 2070 to 2099.

3.3. HWs in Future Climates

3.3.1. Period 2010 to 2039

The number of HWs in the immediate future period of 2010 to 2039 is projected to be higher than the HW frequency in 1983–2012. As expected, the number of HW occurrences are higher during DJF (Figure 7a,b) season in 2010–2039, with areas in the east and northern parts of South Africa projected to experience over 80 events over the 30-year period which is about 10 more than the present-day climate frequency. The simulations for 2010–3039 indicate a slight increase in the overall number of HW frequency in South Africa, particularly across the eastern parts of the country during the JJA season (Figure 8a,b). Simulated HWs under the RCP 4.5 and RCP 8.5 scenarios are in agreement with both sets showing an increase in the events in the future climate. The spatial pattern of simulated HW frequency corresponds closely between the two scenarios for the immediate future period. The western parts of South Africa are simulated to experience the smallest number of HWs (less than 10 events in other areas) over this 30-year period during the austral autumn, winter, and spring. These are the parts influenced the most by passing cold fronts which are responsible for the winter rainfall.

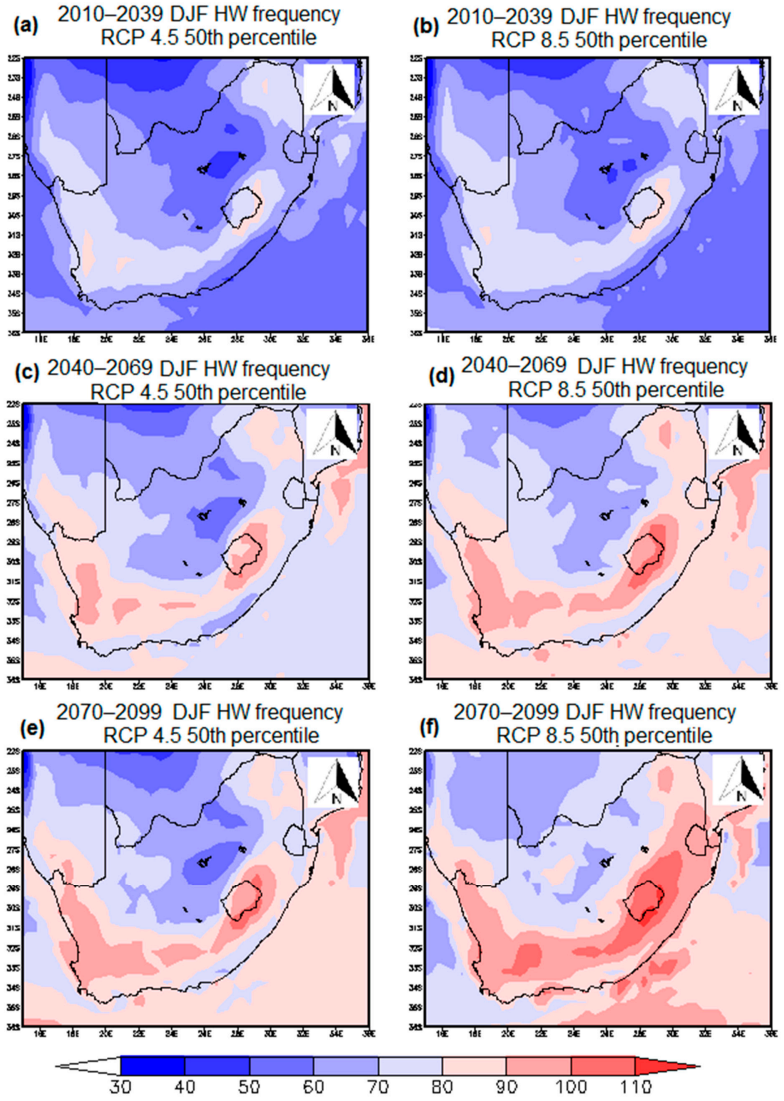

Figure 7. Simulations of DJF HW frequency (total number of occurrence) 50th percentile for (**a**) 2010–2039 RCP 4.5, (**b**) 2010–2039 RCP 8.5, (**c**) 2040-2069 RCP 4.5, (**d**) 2040–2069 RCP 8.5, (**e**) 2070-2099 RCP 4.5 and (**f**) 2070–2099 RCP 8.5.

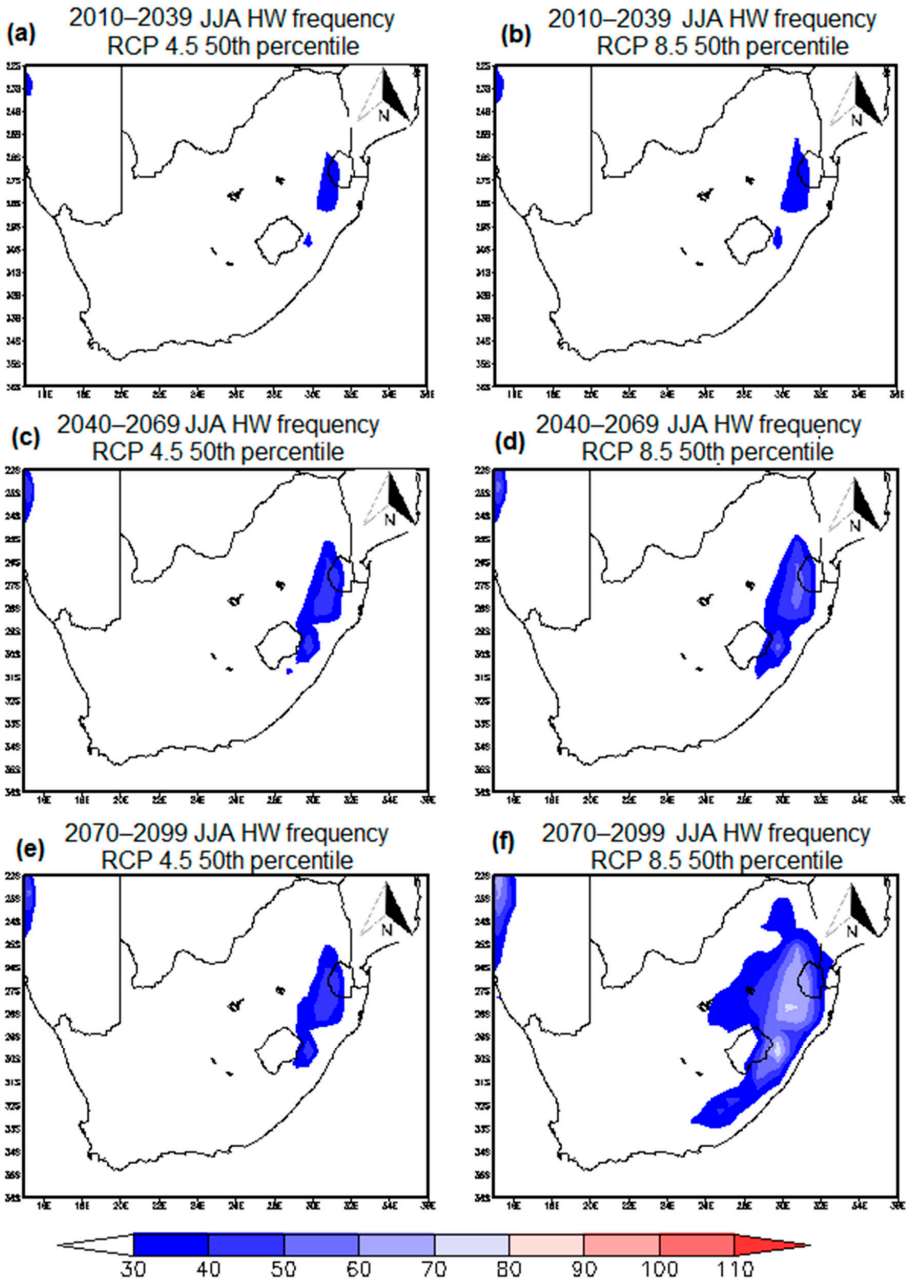

Figure 8. Simulations of JJA HW frequency (total number of occurrence) 50th percentile for (**a**) 2010–2039 RCP 4.5, (**b**) 2010–2039 RCP 8.5, (**c**) 2040–2069 RCP 4.5, (**d**) 2040–2069 RCP 8.5, (**e**) 2070–2099 RCP 4.5 and (**f**) 2070–2099 RCP 8.

The average duration of HWs across South Africa during the 2010–2039 period is projected to increase throughout the year. Regions in the central interior are expected to experience HWs lasting for over a week during SON and DJF. Just like in the present-day-climate, HWs occurring in winter will continue to last for fewer days, i.e., 3–4 days. This is thought to be as a result of the moderating effect by adjacent oceans. HW intensity during this period slightly increases throughout the year compared to the 1983–2012 period. This increase strongly manifests in the 90th percentile under RCP 4.5 and 8.5 in winter with an average increase of about 6°C/30-year period over the Highveld of Mpumalanga and KwaZulu-Natal (not shown). Moreover, the simulation indicates that HWs will be more intense across the north-western part of South Africa during DJF with a seasonal average ranging from 41 to 44 °C during this period.

3.3.2. Period 2040 to 2069

HW frequencies are projected to be significantly higher during this period than during the present-day climate, particularly across the east. Some regions, such as the high-altitude regions of the Free State and KwaZulu-Natal, which were simulated as not experiencing HWs in winter during present-day climate are beginning to experience such events over the mid-future period. Over 20 events are projected to occur across those areas during austral winter.

Dramatic increases in DJF HW frequency are expected during the 2040–2069 period (Figure 7c,d) when compared to the present climate, particularly along the south and eastern coastal regions (frequency of 30 HW higher over the 30-year period). These regions are expected to experience up to 100 events during summer over the 30-year period; which averages to slightly over three events per summer season per year. However, it has to be noted that these HWs are projected to last for less than a week along the coasts but the number of days per event increases inland. Increases in the number of HWs are also observed in a greater extent across the north-western parts of the country during both summer and autumn and the simulations also indicate that 2040–2069 HWs will have the longest duration, between 9 and 10 days, across this region in summer. This may be associated with increasingly dry conditions across this region, as the region experiences little or no rainfall throughout the year. Drier regions heat up quickly because the heating that reaches the surfaces does not start by evaporating water on the surface, which otherwise result in cooling by latent heat absorption [49].

3.3.3. Period 2070 to 2099

HW frequencies are projected to increase across all seasons towards the end of the 21st century. RCP 8.5 indicates higher increases when compared to RCP 4.5 (Figure 7e,f), and the 90th percentile of the ensemble of RCP 8.5 projections also indicate that the eastern half of South Africa may experience up to 60 events in the 2070–2099 30-year period in all seasons; which means 2 HWs per three-month season per year on average. For both DJF and JJA, HW frequency are expected to increase by over 50% in respect to what is experienced in the present-day climate The projected increase is most prominent during the SON (Figure 9a,b) season as most parts that were experiencing HWs less than 20 events in 1983–2012 in the western half of the country are expected to experience over 40 events which is more than 100% increase.

While projected increases during the 2070–2099 period are slightly higher in all seasons compared to the period 2040–2069, major differences in these two periods are observed most strikingly in the average duration of HWs. HW events across coastal and eastern regions of the country are expected to last for about a week (Figure 9c,d). HWs are projected to become common events across South Africa and much of the country's central interior will experience HWs lasting for over 10 days, particularly during summer. As much as simulations indicate that coastal regions will experience most HWs in summer during this 30-year period, the HWs over the coasts will continue to be the least lasting in the country.

HW intensity is projected to drastically increase from the present-day climate towards the end of the 21st century, in the period 2070–2099. The eastern parts of South Africa are expected to experience HWs of low intensity compared to the western parts during summer seasons of the same period. This may be linked to convective rainfall events in the east during SON-DJF, which may bring rainfall and relief to high atmospheric temperatures. However, it is projected that HWs will be more intense on the east particularly across the northeast reaching an average of over 47 °C/30-year period during the March–May (MAM)-JJA compared to the dry western parts of the country (Figure 10).

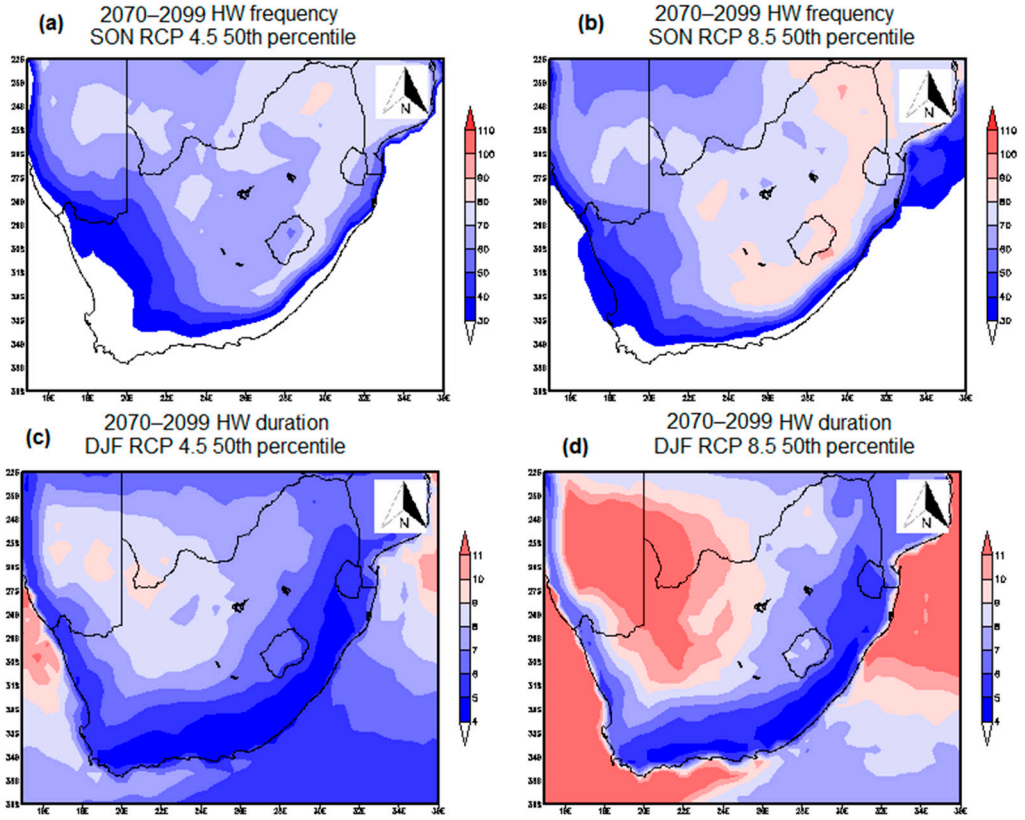

Figure 9. Simulations of SON HW frequency (total number of occurrence) 50th percentile for (**a**) 2070–2099 RCP 4.5, (**b**) 2070–2099 RCP 8.5 and DJF HW average duration 50th percentile (days) for (**c**) 2070–2099 RCP 4.5 and (**d**) 2070–2099 RCP 8.5.

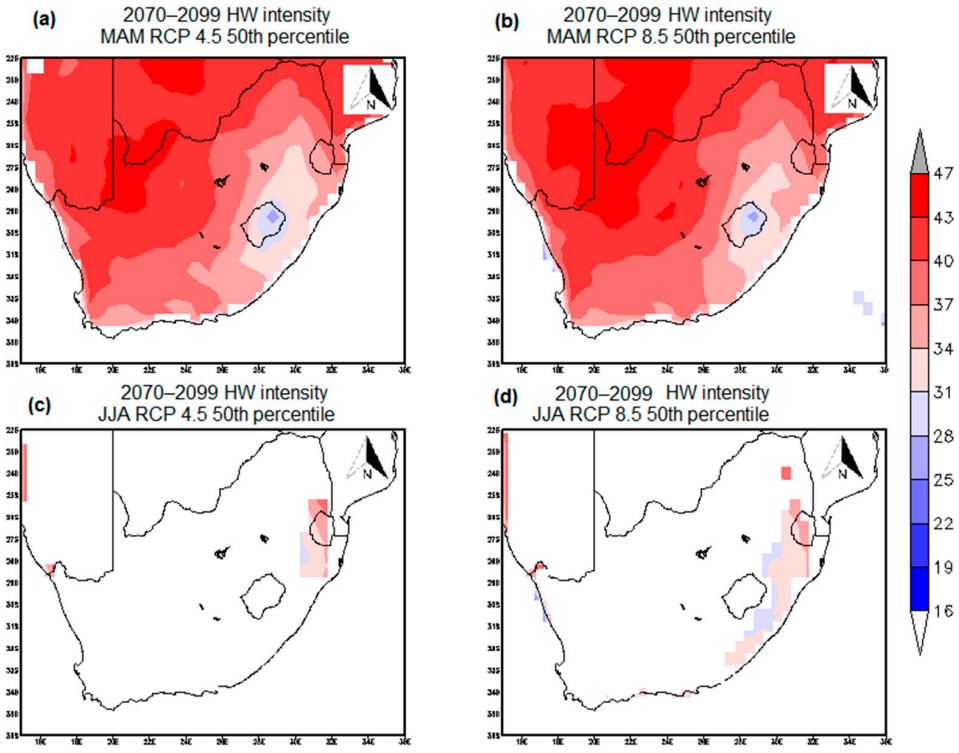

Figure 10. Simulations of HW intensity 50th percentile for (**a**) 2070–2099 MAM RCP 4.5, (**b**) 2070–2099 MAM RCP 8.5, (**c**) 2070–2099 JJA RCP 4.5, and (**d**) 2070–2099 JJA RCP 8.5.

4. Summary and Conclusions

In this study we have shown that there will be a decrease in the number of cold events, while the hot extreme events are increasing. We used an ensemble of CCAM downscalings of six different GCMs for two different RCPs to simulate present-day climate and project changes through to 2099. The HW definition used in this study does not take into account extremes associated with cooler months and changes in impacts associated with adaptation. The simulations were in agreement with observations that the northern parts of the country experiences the highest temperatures, as indicated by the higher number of HW occurrences. The model was, however, found to simulate a high number of total HW occurrences during the present-day climate than those observed, and did not capture the longest lasting HW across the northern parts of Limpopo province. This study has found that HWs are relatively unusual in the present-day climate but are expected to occur more frequently in the future warmer climate when using both RCP 4.5 and RCP 8.5 emission scenarios, particularly during the far future period, 2070–2099, reaching an over 50% increase in both summer and winter. It is also indicated that HWs are also expected to last longer, particularly across the interior, and become more intense, which is in agreement with earlier findings (e.g., [33]) about the nature of HWs in the 21st century.

It has been indicated that, on the global scale, the magnitudes of the probability of climate extremes occurring are expected to change in both mean and variance in the future. It has previously been suggested that, on average, the world is expected to experience more hot weather events [50]. However, that may not be the case on regional basis. Although several studies have investigated temperature projections across Africa (e.g., [5,26]), few studies (e.g., [51,52]) have investigated the attributes and spatial structure of warm temperature extreme events such as HWs in South Africa. In addition to the nature of HWs in the present climate, this study also investigated temperature trends in South Africa in a future warmer climate. During the 2070–2099 period an average increase of 2 HWs per three-month season per year is expected, which is similar to earlier findings [41] that a median increase of 2.5 events per degree of global warming is expected across southern Africa in the 21st century. Simulations indicated that daily maximum temperatures will continue to rise, increasing by up to 6 °C in most parts of the interior of South Africa throughout the year during the 2070-2099 period. This increases the likelihood of having intense and frequent HW occurrences.

Simulated HW thresholds are consistent with observed HW threshold. It was established in this study that HWs will occur more frequent in future climates, especially during DJF season. The simulations also indicate that HW frequency increases with time and last longer, particularly in the interior of South Africa. Regions that are not prone to HW occurrences in the present-day climate are expected to experience HWs in the future warmer climate.

The country experiences less HW events in mid-winter, and that is also expected to continue in future climates. Winter HW events are expected to extend to the eastern interior and to also increase in intensity reaching over 47 °C/30-year. HWs in South Africa are not only increasing in frequency, but are also expected to last longer and become more intense. The increasing intensity is highly indicated under the RCP 8.5 than 4.5. As in the present-day climate, it is also expected that in future climates HWs will last longer, over two weeks in rare circumstances, across the interior of the country compared to coastal regions. In conclusion, HWs in much of South Africa are expected to occur more frequently, last longer, and become more intense.

Author Contributions: Conceptualization, I.M. and M.-J.B.; data curation, F.E.; investigation, I.M. and M.-J.B.; methodology, I.M.; project administration, I.M. and F.E.; supervision, H.C. and N.N.; validation, F.E.; visualization, M.-J.B.; writing—review & editing, H.C. and F.E. All authors have read and agreed to the published version of the manuscript.

Funding: This research received no external funding.

Acknowledgments: South African Weather Service (SAWS) provided observational temperature datasets that were used to calculate HWs in the present-day climate. Council for Scientific and Industrial Research (CSIR) is acknowledged for providing the CCAM model simulations which were performed on the computer clusters of the Centre for High Performance Computing (CHPC). This study was partially supported by generous funding from

South Africa's National Research Foundation (NRF). The authors also acknowledge the centres that ran global models listed in Table 1 used to force the CCAM model.

Conflicts of Interest: The authors declare no conflict of interest.

References

1. Hawkins, E.; Ortega, P.; Suckling, E.; Schurer, A.; Hegerl, G.C.; Jones, P.D.; Joshi, M.; Osborn, T.J.; Masson-Delmotte, V.; Mignot, J.; et al. Estimating changes in global temperature since the pre-industrial period. *Bull. Am. Meteorol. Soc.* **2017**, *98*, 1841–1856. [CrossRef]
2. Masson-Delmotte, V.; Zhai, P.; Pörtner, H.O.; Roberts, D.; Skea, J.; Shukla, P.; Pirani, A.; Moufouma-Okia, W.; Péan, C.; Pidcock, R.; et al. Global Warming of 1.5 °C. 2018. An IPCC Special Report on the Impacts of Global Warming of 1.5 °C Above Pre-Industrial Levels and Related Global Greenhouse Gas Emission Pathways, in The Context of Strengthening the Global Response to the Threat of Climate Change, Sustainable Development, and Efforts to Eradicate Poverty. Available online: https://www.ipcc.ch/sr15/ (accessed on 9 March 2020).
3. Kruger, A.C.; Shongwe, M. Temperature trends in South Africa: 1960–2003. *Int. J. Climatol.* **2004**, *24*, 1929–1945. [CrossRef]
4. MacKellar, N.; New, M.; Jack, C. Observed and modelled trends for rain and temperature for South Africa: 1960–2010. *S. A. J. Sci.* **2014**, *110*. [CrossRef]
5. Engelbrecht, F.A.; Adegoke, J.; Bopape, M.J.; Naidoo, M.; Garland, R.M.; Thatcher, M.; McGregor, J.; Katzfey, J.; Werner, M.; Ichoku, C.; et al. Projections of rapidly rising surface temperatures over Africa under low mitigation. *Environ. Res. Lett.* **2015**, *10*. [CrossRef]
6. Kruger, A.C.; Nxumalo, M.P. Historical rainfall trends in South Africa: 2021–2015. *Water SA* **2017**, *2*, 285–297. [CrossRef]
7. Burls, N.J.; Blamey, R.C.; Cash, B.A.; Swenson, E.T.; Fahad, A.A.; Bopape, M.-J.; Straus, D.M.; Reason, C. The Cape Town "Day Zero" drought and Hadley cell expansion. *NPJ Clim. Atmos. Sci.* **2019**, *2*, 27. [CrossRef]
8. Kruger, A.C.; Sekele, S.S. Trends in extreme temperature indices in South Africa: 1962–2009. *Int. J. Climatol.* **2013**, *33*, 661–676. [CrossRef]
9. Zacharias, S.; Koppe, C.; Mücke, H.G. Climate change effects on HWs and future HW-associated IHD mortality in Germany. *Climate* **2015**, *3*, 100–117. [CrossRef]
10. Min, S.-K.; Zhang, X.; Zwiers, F.W.; Hegerl, G.C. Human contribution to more-intense precipitation extremes. *Nature* **2001**, *470*, 378–381. [CrossRef]
11. Coumou, D.; Rahmstorf, S. A decade of weather extremes. *Nat. Clim. Chang.* **2012**, *2*, 491–496. [CrossRef]
12. Hunt, B.G. A climatology of HWs from a multi-millenial simulation. *J. Clim.* **2007**, *20*, 3802–3821. [CrossRef]
13. Beniston, M. The 2003 HW in Europe: A shape of things to come? An analysis based on Swiss climatological data and model simulations. *Geophys. Res. Lett.* **2004**, *31*, L02202.
14. Cassou, L.; Terray, L.; Phillips, A. Tropical Atlantic influence on European HWs. *J. Clim.* **2005**, *18*, 2805–2811. [CrossRef]
15. Perkins, S.E.; Pitman, A.J.; Sisson, S.A. Systematic differences in 20-year temperature extremes in AR4 model projections over Australia as a function of model skill. *Int. J. Climatol.* **2013**, *33*, 1153–1167. [CrossRef]
16. Nairn, J.; Fawcett, R. *Defining HWs: HW Defined as a Heat Impact Event Servicing all Community and Business Sectors in Australia*; CAWCR Technical Report No. 060; Bureau of Meteorology: Melbourne, Australia, 2013.
17. Boschat, G.; Pezza, A.B.; Simmonds, I.; Perkins, S.E.; Cowan, T.; Purich, A. Large scale and sub-regional connections in the lead up to summer HW and extreme rainfall events in eastern Australia. *Clim. Dyn.* **2014**, *44*. [CrossRef]
18. Vandentorren, S.; Bretin, P.; Zeghnoun, A.; Mandereau-Bruno, L.; Croisier, C.; Riberon, J.; Declercg, B.; Ledrans, M. August 2003 HW in France: Risk factors for death of elderly people living at home. *Eur. J. Public Health* **2006**, *19*, 583–591. [CrossRef]
19. Larsen, J. *Record HW in Europe Takes 35,000 Lives*; Earth Policy Institute: Washington, DC, USA, 2003.
20. Fischer, E.M. The Role of Land–Atmosphere Interactions for European Summer HWs: Past, Present and Future. Ph.D. Thesis, University of Bern, Bern, Switzerland, 2007.
21. Waggoner, P.E. Agriculture and a climate changed by more carbon dioxide. In *National Research Council, Changing Climate. Rep. of the Carbon Dioxide Committee, Board of Atmospheric Sciences and Climate*; National Academy Press: Washington, DC, USA, 1983; pp. 383–418.

22. Maller, C.J.; Strengers, Y. Housing, heat stress and health in a changing climate: Promoting the adaptive capacity of vulnerable households, a suggested way forward. *Health Promot. Int.* **2001**, *26*, 492–498. [CrossRef]
23. Kunkel, K.E.; Changnon, S.A.; Reinke, B.C.; Arritt, R.W. The July 1995 HW in the Midwest: A climatic perspective and critical weather factors. *Bull. Am. Meteorol. Soc.* **1996**, *77*, 1507–1518. [CrossRef]
24. Karl, T.R.; Knight, R.W. The 1995 Chicago HW: How likely a recurrence? *Bull. Am. Meteorol. Soc.* **1997**, *78*, 1107–1119. [CrossRef]
25. Fink, A.H.; Brucher, T.; Kruger, A.; Lackebusch, G.C.; Pinto, J.G.; Ulbrich, U. The 2003 European summer HWs and drought—Synoptic diagnosis and impacts. *Weather* **2004**, *59*, 209–216. [CrossRef]
26. Dosio, A.; Panitz, H.-J. Climate change projections for CORDEX-Africa with COSMO-CLM regional climate model and differences with the driving global climate models. *Clim. Dyn.* **2016**, *46*, 1599–1625. [CrossRef]
27. Russo, S.; Dosio, A.; Graversen, R.G.; Sillmann, J.; Carrao, H.; Dunbar, M.B.; Singleton, A.; Montagna, P.; Barbosa, P.; Vogt, J.V. Magnitude of extreme heat waves in present climate and their projection in a warming world. *J. Geophys. Res. D Atmos.* **2014**, *199*, 500–512. [CrossRef]
28. Godsmark, C.N.; Irlam, J.; van der Merwe, F.; New, M.; Rother, H.-A. Priority focus areas for a sub-national response to climate change and health: A South African provincial case study. *Environ. Int.* **2008**, *128*, 177–184. [CrossRef]
29. Garland, R.; Matoaane, M.; Engelbrecht, E.; Bopape, M.M.; Landman, W.A.; Naidoo, M.; van der Merwe, J.; Wright, C.Y. Regional projections of extreme apparent temperature days in Africa and the related potential risk to human health. *Int. J. Environ. Res. Public Health* **2015**, *12*, 12577–12604. [CrossRef]
30. McGregor, J.L. *C-CAM: Geometric Aspects and Dynamical Formulation. CSIRO Atmospheric Research Tech. Paper No. 70*; CSIRO: Victoria, Australia, 2005; p. 43.
31. McGregor, J.L.; Dix, M.R. An updated description of the conformal cubic atmospheric model. In *High-Resolution Simulation of the Atmosphere and Ocean*; Hamilton, K., Ohfuchi, W., Eds.; Springer: Berlin, Germany, 2008; pp. 51–76.
32. Engelbrecht, F.A.; Landman, W.A.; Engelbrecht, C.J.; Landman, S.; Roux, B.; Bopape, M.J.; Roux, B.; McGregor, J.L. Multi-scale climate modelling over southern Africa using a variable-resolution global model. *Water SA* **2011**, *37*, 647–658. [CrossRef]
33. Fischer, E.M.; Schär, C. Consistent geographical patterns of changes in high-impact European HWs. *Nat. Geosci.* **2010**, *3*, 398–403. [CrossRef]
34. Engelbrecht, F.A.; McGregor, J.L.; Engelbrecht, C. Dynamics of the Conformal-Cubic Atmospheric Model projected climate change signal over southern Africa. *Int. J. Climatol.* **2009**, *29*, 1013–1033. [CrossRef]
35. Rotstayn, L.D. A physically based scheme for the treatment of stratiform clouds and precipitation in large-scale models. I: Description and evaluation of the microphysical processes. *Quart. J. R. Meteorol. Soc.* **1997**, *123*, 1227–1282.
36. McGregor, J.L. A new convection scheme using a simple closure. *Curr. Issues Parameter. Convect.* **2003**, *93*, 33–36.
37. McGregor, J.L.; Gordon, H.B.; Watterson, I.G.; Dix, M.R.; Rotstayn, L.D. *The CSIRO 9-level Atmospheric General Circulation Model. CSIRO Div. Atmospheric Research Tech*; CSIRO: Victoria, Australia, 1993; p. 89.
38. Holtslag, A.A.M.; Boville, B.A. Local versus nonlocal boundary-layer diffusion in a global climate model. *J. Clim.* **1993**, *6*, 1825–1842. [CrossRef]
39. *IPCC: Climate Change. Synthesis Report. Contribution of Working Groups I, II and III to the Fifth Assessment Report of the Intergovernmental Panel on Climate Change*; Core Writing Team; Pachauri, P.K.; Meyer, L.A. (Eds.) IPCC: Geneva, Switzerland, 2014; p. 151.
40. Meehl, G.A.; Tebaldi, C. More intense, more frequent, and longer-lasting HWs in the 21st century. *Science* **2004**, *305*, 994–997. [CrossRef] [PubMed]
41. Zhang, X.; Yang, F. RClimDex (1.0), User Manual, Climate Research Branch, Environment Canada, Downsview, Ontario, Canada. 2004. Available online: http://cccma.seos.uvic.ca/ETCCDMI (accessed on 5 November 2015).
42. CCDI/CRD Climate Change Indices. Available online: http://etccdi.pacificclimate.org/software.shtml (accessed on 28 April 2020).
43. Dix, M.; Vohralik, P.; Bi, D.; Rashid, H.; Marsland, S.; O'Farrell, S.; Uotila, P.; Hirst, T.; Kowalczyk, E.; Sullivan, A.; et al. The ACCESS couple model: Documentation of core CMIP5 simulations and initial results. *Aust. Meteorol. Oceanogr. J.* **2013**, *63*, 83–99. [CrossRef]

44. Gent, P.R.; Danabasoglu, G.; Donner, L.J.; Holland, M.M.; Hunke, E.C.; Jayne, S.R.; Lawrence, D.M.; Neale, R.B.; Rasch, P.J.; Vertenstein, M.; et al. The community climate system model version 4. *J. Clim.* **2011**, *24*, 4973–4991. [CrossRef]
45. Griffies, S.M.; Winton, M.; Donner, L.J.; Horowitz, L.W.; Downes, S.M.; Farneti, R.; Gnanadesikan, A.; Hurlin, W.J.; Lee, H.-C.; Liang, Z.; et al. GFDL's CM3 coupled climate model: Characteristics of the ocean and sea ice simulations. *J. Clim.* **2011**, *24*, 3520–3544. [CrossRef]
46. Giorgetta, M.A.; Jungclaus, J.; Reick, C.H.; Legutke, S.; Bader, J.; Bottinger, M.; Brovkin, V.; Crueger, C.; Esch, M.; Fieg, K.; et al. Climate and carbon cycle changes from 1850 to 2100 in MPI-ESM simulations for the Coupled Model Intercomparison Project phase 5. *J. Adv. Model. Earth Syst.* **2013**, *5*, 572–597. [CrossRef]
47. Bentsen, M.; Bethke, I.; Debernard, J.B.; Iversen, T.; Kirkevåg, A.; Seland, Ø.; Drange, H.; Roelandt, C.; Seierstad, I.A.; Hoose, C.; et al. The Norwegian Earth System Model, NorESM1-M—Part 1: Description and basic evaluation of the physical climate. *Geosci. Model. Dev.* **2013**, *6*, 687–720. [CrossRef]
48. Salas-Mélia, D.F.; Chauvin, M.; Déqué, H.; Douville, H.; Gueremy, J.-F.; Marquet, P.; Planton, S.; Royer, J.F.; Tyteca, S. Description and validation of the CNRM-CM3 global coupled model. *Clim. Dyn.* **2005**, *103*.
49. Fischer, E.M.; Schär, C. Future changes in daily summer temperature variability: Driving processes and role for temperature extremes. *Clim. Dyn.* **2009**, *33*, 917–935. [CrossRef]
50. IPCC. *Climate Change. The Scientific Basis. Contribution of Working Group I to the Third Assessment Report of the Intergovernmental Panel on Climate Change*; Cambridge University Press: Cambridge, UK; New York, NY, USA, 2001.
51. Russo, S.; Marchese, A.F.; Sillmann, J.; Immé, G. When will unusual heat waves become normal in a warming Africa? *Environ. Res. Lett.* **2016**, *11*, 054016. [CrossRef]
52. Perkins-Kirkpatrick, S.E.; Gibson, P.B. Changes in regional heatwave characteristics as a function of increasing global temperature. *Sci. Rep.* **2017**, *7*, 12256. [CrossRef]